Biochimica et Biophysica Acta 1850 (2015) 97–106

Contents lists available at ScienceDirect

Biochimica et Biophysica Acta

journal homepage: www.elsevier.com/locate/bbagen

# Free-radical first responders: The characterization of CuZnSOD and MnSOD regulation during freezing of the freeze-tolerant North American wood frog, *Rana sylvatica*

Neal J. Dawson, Barbara A. Katzenback, Kenneth B. Storey *

*Department of Biology and Institute of Biochemistry Carleton University, Ottawa, ON, Canada*

ARTICLE INFO

*Article history:*
Received 22 May 2014
Received in revised form 3 October 2014
Accepted 6 October 2014
Available online 12 October 2014

*Keywords:*
*Rana sylvatica*
Freeze tolerance
Ischemia
Oxidative stress
Antioxidant
Protein stability

ABSTRACT

*Background:* The North American wood frog, *Rana sylvatica*, is able to overcome subzero conditions through overwintering in a frozen state. Freezing imposes ischemic and oxidative stress on cells as a result of cessation of blood flow. Superoxide dismutases (SODs) catalyze the redox reaction involving the dismutation of superoxide ($O_2^{-\bullet}$) to molecular oxygen and hydrogen peroxide.
*Methods:* The present study investigated the regulation of CuZnSOD and MnSOD kinetics as well as the transcript, protein and phosphorylation levels of purified enzyme from the muscle of control and frozen *R. sylvatica*.
*Results:* CuZnSOD from frozen muscle showed a significantly higher $V_{max}$ (1.52 fold) in comparison to CuZnSOD from the muscle of control frogs. MnSOD from frozen muscle showed a significantly lower $K_m$ for $O_2^{-\bullet}$ (0.66 fold) in comparison to CuZnSOD from control frogs. MnSOD from frozen frogs showed higher phosphorylation of serine (2.36 fold) and tyrosine (1.27 fold) residues in comparison to MnSOD from control animals. Susceptibility to digestion via thermolysin after incubation with increasing amount of urea ($C_m$) was tested, resulting in no significant changes for CuZnSOD, whereas a significant change in MnSOD stability was observed between control (2.53 M urea) and frozen (2.92 M urea) frogs. Expressions of CuZnSOD and MnSOD were quantified at both mRNA and protein levels in frog muscle, but were not significantly different.
*Conclusion:* The physiological consequence of freeze-induced SOD modification appears to adjust SOD function in freezing frogs.
*General significance:* Augmented SOD activity may increase the ability of *R. sylvatica* to overcome oxidative stress associated with ischemia.



## 1. Introduction

The North American wood frog, *Rana sylvatica*, is a unique terrestrial frog that overwinters in a whole animal frozen state, in which as much as 65–70% of the frog's total body water is converted into extracellular ice [1]. In a frozen state, cells are exposed to ischemic conditions as a result of a cessation in cardiac function and blood flow [1,2]. Wood frogs cope with freezing/ischemic defense by (a) employing metabolic rate depression to reduce overall energy demands, (b) sustaining elevated constitutive levels of antioxidants and antioxidant enzymes in their tissues and (c) increasing the total antioxidant capacity by increasing select antioxidant enzymes including superoxide dismutase (SOD), glutathione peroxidase, glutathione-S-transferase, catalase, and glutathione reductase [3,4]. It is apparent that antioxidant defenses are critical for entry and exit from hypometabolism to deal with changes in oxygen consumption and generation of reactive oxygen species (ROS), such as during wood frog freezing.

*Abbreviations:* ALS, amyotrophic lateral sclerosis; AMPK, 5′ adenosine monophosphate-activated protein kinase; $C_m$, the denaturant concentration at which half of the protein is unfolded; CuZnSOD, copper and zinc containing SOD; $DEAE^+$, diethylaminoethyl cellulose; DEPC, diethylpyrocarbonate; DTT, dithiothreitol; FeSOD, iron containing superoxide dismutase; $K_m$, Michaelis–Menten constant; IMAC, immobilized metal ion affinity chromatography; $IP_3$, inositol trisphosphate; KPi, potassium phosphate; MAPK, mitogen activated protein kinase; MnSOD, manganese containing superoxide dismutase; NBT, nitrotetrazolium blue; NiSOD, nickel containing superoxide dismutase; PKA, protein kinase A; PKC, protein kinase C; PKG, protein kinase G; PMSF, phenylmethylsulfonyl fluoride; PP1, protein phosphatase 1; PP2A, protein phosphatase 2A; PP2C, protein phosphatase 2C; PVDF, polyvinylidene difluoride; ROS, reactive oxygen species; TBST, Tris buffered saline with Tween; $V_{max}$, maximal velocity

* Corresponding author at: Institute of Biochemistry and Department of Biology, 1125 Colonel By Drive, Carleton University, Ottawa, ON K1S 5B6, Canada. Tel.: +1 613 520 3678; fax: +1 613 520 3749.
*E-mail address:* kenneth_storey@carleton.ca (K.B. Storey).

http://dx.doi.org/10.1016/j.bbagen.2014.10.003
0304-4165/

The importance of antioxidant enzymes for freeze tolerance stems from the buildup of ROS during, and upon exit from, ischemic events [5]. Superoxide dismutases (SODs, E.C. 1.15.1.1) are crucial enzymes involved in the mitigation of oxidative damage by catalyzing the disproportionation of superoxide ($O_2^{-\bullet}$) into oxygen and hydrogen peroxide. Specifically, SOD catalyzes the following reactions:

$$\text{M (ox)-SOD} + O_2^{-\bullet} \rightarrow \text{M (red)-SOD} + O_2$$

$$\text{M (red)-SOD} + O_2^{-\bullet} + 2H^+ \rightarrow \text{M (ox)-SOD} + H_2O_2$$

(where M = Cu(II/I) or Mn(II/I)).

$O_2^{-\bullet}$ is one of the main reactive oxygen species found ubiquitously across tissues and organisms. There are several forms of SOD found in nature, these unique metalloproteins are identified through their metal cofactors: 1) copper and zinc containing SOD (CuZnSOD) is typically found in the cytosol of nearly all eukaryotic cells; 2) manganese SOD (MnSOD) is found in the mitochondria or peroxisomes, or 3) nickel (NiSOD) or iron (FeSOD) containing SODs are typically found in prokaryotes, protists and select eukaryotes [6–9]. Of the many forms of SOD, only CuZnSOD and MnSOD are known to exist in frogs [10–13]. It has been suggested that the cytoplasmic form, CuZnSOD, acts like a buffer against the buildup of intracellular $O_2^{-\bullet}$, whereas the mitochondrial form, MnSOD, plays a pivotal role in the disproportionation of the large amount of $O_2^{-\bullet}$ generated by the electron transport chain housed within the mitochondria [14,15]. CuZnSOD and MnSOD have been sequenced from the African clawed frog, *Xenopus laevis*, and exist as homodimers with molecular weights of approximately 32 kDa and 46 kDa, respectively [10,13]. Studies have shown the importance of functional CuZnSOD as many disease states can be attributed to mutations in the *sod1* gene [16]. The role of MnSOD in disease states is less characterized as knockout experiments involving *sod2* are lethal [14,17–19].

SODs have been widely studied and characterized from traditional animal models (human, rat mouse), however, less is known about the role of SODs in aiding survival of the freeze tolerant frog. Reversible protein phosphorylation continues to emerge as an increasingly common method of posttranslationally modifying and regulating enzymes within freeze-tolerant animals. There is evidence to support the posttranslational modification of enzymes such as protein kinases, phosphatases, and metabolic enzymes via reversible phosphorylation as a potential control mechanism for altering enzymatic activity in *R. sylvatica* in response to freezing in the muscle [20–28]. This manuscript presents the first investigation of the potential regulation of CuZnSOD and MnSOD separately in the leg muscle of *R. sylvatica* comparing control and frozen states, and provides evidence for post-translational modification as the mechanism of enzyme regulation to aid successful overwintering of the frog.

## 2. Materials and methods

### 2.1. Chemicals

All biochemicals were from BioShop (Burlington, ON, Canada) with a few exceptions; xanthine and xanthine oxidase were from Sigma (St. Louis, MO), immobilized metal ion affinity chromatography (IMAC) chelating fast flow column was from Pharmacia (Uppsala, SE), and potassium phosphate, monobasic was from J.T. Baker Chemical Company (London, UK).

### 2.2. Animals

Male wood frogs were obtained from the Ottawa area and were washed in a tetracycline bath before being placed in plastic containers with damp sphagnum moss at 5 °C for one week. Control frogs were sampled from this condition. Frogs were exposed to freezing conditions for 24 h as previously described [29,30]. Control and frozen frogs were euthanized by pithing. Muscle tissues were quickly excised and flash frozen in liquid $N_2$. All tissue samples were stored at −80 °C until use. The Carleton University Animal Care Committee, in accordance with the Canadian Council on Animal Care guidelines, approved all animal handling protocols used during this study.

### 2.3. Preparation of muscle tissue lysates for protein purification

For protein purification, samples of frozen muscle tissue were homogenized 1:5 w/v in ice-cold homogenizing buffer A [20 mM potassium phosphate (KPi) buffer, pH 7.2, containing 15 mM β-glycerophosphate, 1 mM EGTA, 1 mM EDTA, 5% v/v glycerol and 1 mM phenylmethylsulfonyl fluoride (PMSF)]. Homogenates were then centrifuged at 13,500 ×*g* at 4 °C for 30 min and the supernatants collected for use in protein purification.

### 2.4. Preparation of muscle tissue lysates for determination of relative protein levels

Samples of muscle tissue were crushed under liquid nitrogen and then homogenized 1:2.5 w/v in homogenizing buffer B (20 mM HEPES, pH 7.5, 200 mM NaCl, 0.1 mM EDTA, 10 mM NaF, 1 mM $Na_3VO_4$, 10 mM β-glycerophosphate) with a few crystals of PMSF and 1 μL/mL Sigma protease inhibitor cocktail (104 mM AEBSF, 80 μM Aprotinin, 4 mM Bestatin, 1.4 mM E-64, 2 mM Leupeptin, 1.5 mM Pepstatin A). Samples were homogenized on ice with a Polytron PT1000 homogenizer and centrifuged at 4 °C for 15 min at 10,000 ×*g*. Soluble protein concentrations were assessed using the BioRad protein assay with bovine serum albumin (BSA) used as the standard curve according to the manufacturer's instructions. All samples were adjusted to 10 μg/μL by adding a calculated small volume of homogenizing buffer B. Aliquots of samples were then mixed 1:1 v/v with 2× SDS loading buffer (100 mM Tris-base, 4% w/v SDS, 20% v/v glycerol, 0.2% w/v bromophenol blue, 10% v/v 2-mercaptoethanol). Final sample concentrations were 5 μg/μL. Proteins were denatured by placing the tubes in boiling water for 5 min. Samples were stored at −80 °C until use.

### 2.5. Purification of CuZnSOD and MnSOD

A 3 mL aliquot of crude supernatant was applied to a $DEAE^+$ column (1.5 cm × 20 cm), previously equilibrated with 50 mL of homogenization buffer A. The $DEAE^+$ column was then washed with 50 mL of buffer A to remove unbound protein. SOD was eluted from the $DEAE^+$ column with a linear gradient of 0–1 M KCl in homogenization buffer A. Fractions of 1.24 mL were collected and 5 μL from each fraction was assayed to detect SOD activity (see Kinetic assays section below for methodology). The fractions of peak SOD activity were pooled and applied to Sephadex G-50 gel buffer exchange columns equilibrated with buffer C (20 mM KPi buffer, pH 7.2 containing 15 mM β-glycerophosphate, 5% v/v glycerol). A 5 cm column of Sephadex G-50 in a syringe barrel was equilibrated in buffer C and centrifuged at 500 ×*g* in a bench-top centrifuge for 2 min to remove excess buffer. A 500 μL aliquot of SOD eluant was applied to each buffer exchange column and centrifuged again. The resulting eluant was collected and applied to an IMAC column pre-charged with 1 mg/mL $CuSO_4 \cdot H_2O$ (1.5 cm × 10 cm), equilibrated in homogenization buffer C. The copper chelate affinity column was then washed with 50 mL of homogenization buffer C to remove unbound protein. Bound proteins were eluted with a linear gradient of 0–1 M KCl in homogenization buffer A. Fractions of 1.24 mL were collected and 10 μL from each fraction was assayed to detect SOD activity. Fractions containing the highest SOD activity from the copper chelate affinity column were pooled and used for further

study. The purity of SOD was determined by combining samples with an equal volume of 2× SDS loading buffer, boiling for 5 min, and then running 20 μL of sample purified from each successive purification on SDS-PAGE gels (see below Gel electrophoresis and Western blotting section). Protein banding was visualized with Coomassie blue.

### 2.6. Kinetic assays

SOD activity was assayed based on the generation of superoxide radicals formed by xanthine and xanthine oxidase: 100 mM KPi buffer (pH 7.4), 1 mM xanthine, 2 U xanthine oxidase, and 2 mM nitrotetrazolium blue (NBT). This assay mixture generates $O_2^{-\bullet}$, which oxidizes NBT to form formazan dye. SOD (contained within the tissue homogenate supernatant) inhibits the oxidation of NBT by catalyzing the dismutation of $O_2^{-\bullet}$ generated in the xanthine oxidase reaction. One unit of enzyme activity is the amount of SOD that inhibits the reduction of nitrotetrazolium blue by 50% at 25 °C. Assays were blanked by subtracting the spontaneous reduction of NBT oxidation from the measured values. The formation of formazan was measured at 545 nm in a Thermo Labsystems Multiskan spectrophotometer (Thermo Scientific, Waltham, MA, USA). Data were analyzed using the Kinetics v.3.5.1 program [31].

### 2.7. RNA isolation

Total RNA from frog muscle tissues was extracted using TRIzol™ reagent (Invitrogen) according to the manufacturer's instructions and as described previously [30]. The RNA concentration of each sample was determined on a GeneQuant Pro spectrophotometer (Pharmacia, Markham, Ontario, Canada) at 260 nm. RNA purity was assessed using a ratio of absorbance at 260/280 nm, while RNA quality was examined by observing the integrity of 18S and 28S ribosomal RNA (rRNA) bands on a native agarose gel following electrophoresis with SYBR green staining. Total RNA was isolated from the muscle of 4–5 control frogs and 4–5 frozen frogs for use in cDNA synthesis.

### 2.8. cDNA synthesis

Five μg of total RNA in a volume of 10 μL was used for first strand cDNA synthesis. One μL of oligo-dT (200 ng/μL; 5′-TTTTTTTTTTTTTTT TTTTTV-3′; V = A or G or C) (Sigma Genosys) was added to each sample before samples were incubated at 65 °C for 5 min in a thermocycler (Mastercycler Eppendorf) and then chilled on ice for 5 min. Four μL of 5× first strand buffer (Invitrogen), 2 μL 100 mM DTT (Invitrogen), 1 μL 10 mmol/L dNTPs (Bio Basic), and 1 μL Superscript II reverse transcriptase (Invitrogen) were added to each reaction and further incubated at 42 °C for 45 min in an Eppendorf thermocycler (Mississauga, Ontario, Canada). Synthesized cDNA samples were stored at −20 °C until use.

### 2.9. RT-PCR

Synthesized cDNA samples were checked for potential genomic contamination using the *α-tubulin* primer set that was designed to span an intron. All cDNA samples were negative for genomic contamination. For gene expression studies, serial dilutions of cDNA ($10^{-1}$ and $10^{-2}$) were made to identify the dilution that produced non-saturating yet visible bands for the gene of interest following PCR amplification for quantification purposes. The primer sequences for target genes were (1) *sod1* sense 5′-tgaaggcvgtgtgtgtghtgaaggga-3′, antisense 5′-ccaatnacdccacaagccaracg-3′, (2) *sod2* sense 5′-ctggacaaacctctctccta-3′, antisense 5′-cttgtaagcggttagattctttg-3′, and (3) *α-tubulin* sense 5′-aaggaagatgctgccaataa-3′, antisense 5′-ggtcacat ttcaccatctg-3′.

PCR reactions consisted of 5 μL of diluted cDNA, 15 μL of DEPC treated water, 1.25 μL of primer mixture (0.03 nmol/μL), 0.75 μL of 10× PCR buffer (Invitrogen), 1.5 μL of 50 mmol/L $MgCl_2$, 0.5 μL of 10 mmol/L dNTPs, and 1 μL of *Taq* polymerase. Thermocycling conditions were: (1) 10 min at 94 °C, 20 cycles of 94 °C for 30 s, 56 °C for 30 s, and 72 °C for 45 s for *sod1*, (2) 10 min at 94 °C, 24 cycles of 94 °C for 30 s, 62 °C for 30 s, and 72 °C for 45 s for *sod2*, or (3) 10 min at 94 °C, 22 cycles of 94 °C for 30 s, 53.2 °C for 30 s, and 72 °C for 45 s for *α-tubulin*. All thermocycling protocols included a final elongation of 72 °C for 7 min. Following amplification, 3 μL of DNA loading dye [1 μL 2× SYBR® Green I nucleic acid gel stain (Invitrogen) + 2 μL of loading buffer (0.25% bromophenol blue, 0.25% xylene cyanol FF, and 40% sucrose in $ddH_2O$)] was added to each PCR reaction. A 14 μL aliquot of each sample was loaded into 1.5% (*α-tubulin* and *sod1*) or 2.0% (*sod2*) agarose gels and electrophoresed in 1× TAE buffer (2 mol/L Tris base, 1.1 mL acetic acid/L, 1 mmol/L EDTA, pH 8.5) at 130 V for 25–30 min. PCR-amplified products were visualized using the Chemi-Genius BioImaging system. The intensity of the *sod1* or *sod2* PCR products was expressed as a ratio against the corresponding band intensities of *α-tubulin* amplified from the same cDNA sample to correct for any minor variations in sample loading. The ratio of target gene to the reference gene (*α-tubulin*) from the muscle of control frogs was set to a reference value of 1, to which the relative mRNA levels of the target gene in the muscle of frozen frogs were expressed as a fold change. Each data bar represents the means ± s.e.m. derived from n = 4–5 different animals per group.

The PCR products were isolated from gel slices using the freeze/squeeze method and sequenced at Bio Basic (Markham, ON, Canada) as previously described [30]. Sequence identities were confirmed by sequence comparison in BLASTn.

### 2.10. Gel electrophoresis and Western blotting

Protein separation was achieved by running samples on 12% (samples from protein purification steps) or 15% (samples from protein stability assays or from tissue lysates) SDS-PAGE gels. Sample aliquots were loaded onto polyacrylamide gels together with pre-stained molecular weight standards (FroggaBio; Cat. # PM005-0500) and separated using a discontinuous buffer system. Electrophoresis was carried out at 185 V for 45 min using the BioRad Mini-Protean 3 system with 1× Tris–glycine running buffer. Proteins on the gel were then electroblotted onto polyvinylidene difluoride (PVDF) membrane (Millipore, Bedford, MA) using a BioRad mini Trans-Blot cell. The transfer was carried out at 160 mA for 1.5 h. Following the transfer, membranes were washed in TBST (10 mM Tris, pH 7.5, 150 mM NaCl, 0.05% v/v Tween-20) for 3× 5 min. The membranes were blocked using 2.5% skim milk in TBST for 30 min. After blocking, the membranes were probed with primary antibody diluted 1:1000 v:v for CuZnSOD or 1:2000 v:v for MnSOD in TBST for 3 h at room temperature (RT). Primary antibodies were rabbit anti-SOD1 (GenScript, A01005) and rabbit anti-SOD2 (Stress Marq BioSciences, SPC-118C). The membranes were washed 3× 5 min with TBST at RT and probed with goat anti-rabbit-peroxidase secondary antibody for 30 min. Membranes were washed again 3× 5 min in TBST at RT and developed using enhanced chemiluminescence.

SOD1 and SOD2 antibodies cross-reacted with bands corresponding to molecular weights of ~15 kDa and ~26 kDa, respectively. Blots were developed with enhanced chemiluminescence reagents. Images were captured using a ChemiGenius Bio-Imaging system with GeneSnap software and densitometry analysis performed using GeneTools software (Syngene, Frederick, MD). The intensity of the immunoreactive bands was standardized against a group of at least 3 bands, not located close to the band of interest, in the corresponding Coomassie blue stained membrane. The intensity of the immunoreactive bands from control muscle tissue was set to a reference value of 1 to which the intensity of standardized immunoreactive bands from frozen muscle tissue was expressed as a fold change.

### 2.11. ProQ Diamond phosphoprotein staining

Enzyme extracts from both control and frozen frog muscle for MnSOD and CuZnSOD were purified as described in Section 2.5. The top three fractions based on activity were pooled and protein levels in the pooled fractions were quantified using the Coomassie blue dye-binding method. Aliquots of the pooled fractions were then mixed 1:1 v/v with 2× SDS loading buffer (100 mM Tris buffer, pH 6.8, 4% w/v SDS, 20% v/v glycerol, 0.2% w/v bromophenol blue, 10% v/v 2-mercaptoethanol) and subsequently boiled for 5 min and stored at −20 °C until used.

Equal volumes of each sample were loaded on a 12% SDS-PAGE gel. The gel was run at 185 V for 45 min in running buffer (0.5 M Tris, 5 M glycine, 0.5% w/v SDS). The gel was removed and washed in fixing solution (50% v/v methanol, 10% v/v acetic acid) twice for 10 min, then left in fixing solution overnight at 4 °C followed by 3 washes with $ddH_2O$ for 10 min. The gel was then stained with ProQ Diamond phosphoprotein stain (Invitrogen, Eugene, OR) for 90 min and washed 3 times with $ddH_2O$ for 10 min. The gel was covered during staining (and for the remainder of the protocol) with aluminum foil to prevent the photosensitive stain from interacting with light. To minimize non-specific background, the gel was washed in ProQ Diamond destaining solution (20% v/v acetonitrile, 50 mM sodium acetate, pH 4) for 45 min, and washed 3 times in $ddH_2O$ for 10 min. Gels were stained with Coomassie blue to account for any discrepancies in gel loading. Bands on the gel were then visualized using the ChemiGenius Bio-Imaging system with GeneSnap software and quantified using GeneTools software (Syngene, Frederick, MD) by calculating the ratio of phosphoprotein stain, to protein content determined by Coomassie blue staining.

### 2.12. Dot blotting

The phosphorylation of MnSOD was further assessed by applying equal amounts of purified enzyme from the muscle of control and frozen frogs onto nitrocellulose membranes (Bio-Rad, Hercules, CA, USA) using a Bio-Dot micro-filtration apparatus (Bio-Rad, Hercules, CA, USA), as previously described [32]. Primary antibodies (diluted 1:1000 v/v) were then applied to different wells and membranes were allowed to incubate overnight at 4 °C with gentle rocking. Primary antibodies used were: (1) rabbit anti-phosphoserine (Cat. # 618100, Invitrogen, Carlsbad, CA, USA); (2) rabbit anti-phosphothreonine (Cat. # 718200, Invitrogen, Carlsbad, CA, USA); or (3) rabbit anti-phosphotyrosine (Cat. # 615800, Invitrogen, Carlsbad, CA, USA). Dots on the membrane were then visualized using the ChemiGenius Bio-Imaging system with GeneSnap software and quantified using GeneTools software (Syngene, Frederick, MD) by calculating the ratio of antibody signal, to protein content determined by Coomassie blue staining.

### 2.13. Determination of protein stability

Frog muscle tissue was homogenized as previously described in Section 2.3, without the use of PMSF. To assess the possibility of structural/conformational changes in CuZnSOD or MnSOD between the control and 24 h frozen conditions, the susceptibility of both forms of SOD to denaturation by urea (0–7 M) was evaluated. Four separate preparations of crude muscle extracts were incubated with different concentrations of urea for 24 h at 4 °C in buffer A in the absence of PMSF. After incubation, each sample was subjected to pulse proteolysis as outlined by Park and Marqusee [33] to cleave unfolded, denatured enzyme. To do this, thermolysin (0.40 mg/mL in 50 mM Tris, pH 8.0, 2.5 M NaCl, 10 mM $CaCl_2$) was added to initiate proteolysis. Various incubation times with thermolysin were explored to discover the optimum amount of digestion time required, resulting in the use of a 30 min incubation optimum. Following a 30 min pulse reaction time at 4 °C, the reaction was quenched by mixing samples 5:1 v/v with 6× SDS loading buffer (375 mM Tris buffer, pH 6.8, 9% w/v SDS, 50% v/v glycerol, 0.03% w/v bromophenol blue, 10% v/v 2-mercaptoethanol) and subsequently boiled for 5 min and stored at −20 °C until used. Western blotting was then performed as above and CuZnSOD and MnSOD band intensities were quantified to reveal the amount of undigested enzyme remaining. From this, $C_m$ values were calculated, representing the amount of urea that reduced the amount of folded protein by one-half.

### 2.14. Statistical analysis

Comparison of enzyme kinetics, relative protein and mRNA levels was performed using a Student's *t*-test, two-tailed, assuming unequal variances. A probability of $p < 0.05$ was considered significant.

## 3. Results

### 3.1. Purification of CuZnSOD and MnSOD from the muscle of control and frozen frogs

The purification schemes used for wood frog muscle CuZnSOD and MnSOD are shown in Tables 1 and 2, respectively. The procedure used ion exchange chromatography on DEAE Sephadex (Fig. 1A), a buffer exchange step to remove EDTA/EGTA, and copper chelate affinity chromatography. The buffer exchange step was crucial to this purification procedure, since the EGTA and EDTA that were in homogenization buffer A caused the copper to dissociate from the copper chelate column. CuZnSOD eluted from the copper chelate affinity column at approximately 200 mM KCl whereas MnSOD eluted at approximately 400 mM KCl (Fig. 1B). Frog muscle CuZnSOD was purified 209 fold with an overall yield of activity of 10.8% (Table 1). The final specific activity of CuZnSOD was 1390 U/mg protein (Table 1). Frog muscle MnSOD was purified 234 fold with an overall yield of activity of 20.1% (Table 2). The final specific activity of MnSOD was 1550 U/mg protein (Table 2). The success of the purification process was assessed by Western blotting on all fractions containing SOD activity with antibodies for CuZnSOD and MnSOD enzymes (Fig. 2). The purification resulted in one band corresponding to correct molecular weight of ~15 kDa for CuZnSOD and ~26 kDa for MnSOD (Fig. 3).

### 3.2. Kinetic characterization of CuZnSOD and MnSOD

Kinetic parameters of purified muscle SOD were assessed to determine if the enzyme's properties differed between control and frozen animals. For both CuZnSOD and MnSOD, kinetic parameters changed during freezing in comparison to the control enzyme ($p < 0.05$) (Table 3). The frozen form of MnSOD had an apparent $K_m$ for xanthine that was 34% lower than the control enzyme. In the case of CuZnSOD, however, there was no significant change in the apparent $K_m$ of xanthine between control and frozen groups. In all cases, blanks were run to test for reactivity between purified enzyme and NBT reduction. Background activity was subtracted from the final observed rates of superoxide scavenging. The $V_{max}$ did not change significantly for MnSOD in frozen muscle in comparison to control

**Table 1**
Typical purification and yield of *Rana sylvatica* muscle CuZnSOD.

| Purification step | Total protein (mg) | Total activity (U) | Specific activity (U/mg) | Fold purification | Yield (%) |
|---|---|---|---|---|---|
| Crude extract | 185.6 | 1230 | 6.6 | – | 100 |
| $DEAE^+$ | 9.0 | 837 | 93.1 | 14.0 | 68.1 |
| Copper chelate | 0.096 | 133 | 1390 | 209.0 | 10.8 |

**Table 2**
Typical purification and yield of *Rana sylvatica* muscle MnSOD.

| Purification step | Total protein (mg) | Total activity (U) | Specific activity (U/mg) | Fold purification | Yield (%) |
|---|---|---|---|---|---|
| Crude extract | 185.6 | 1230 | 6.6 | – | 100 |
| DEAE$^+$ | 9.0 | 837 | 93.1 | 14.0 | 68.1 |
| Copper chelate | 0.16 | 247 | 1550 | 234.0 | 20.1 |

muscle tissue; however, there was a significant 1.52 fold increase in the $V_{max}$ for CuZnSOD during freezing (Table 3).

### 3.3. mRNA levels of sod1 and sod2

Using homology based primers, partial sequences for *sod1* and *sod2* in *R. sylvatica* were obtained. The partial sequences of *R. sylvatica sod1* and *sod2* were submitted to NCBI GenBank, accession numbers KJ847420 and KJ87421, respectively. The *R. sylvatica sod1* partial open reading frame was 392 bp, corresponding to 130 amino acids (representing 84.4% of the 154 aa of human CuZnSOD, 86.6% of 150 aa of *Rana catesbeiana* CuZnSOD, 86.1% of 151 aa of *Xenopus tropicalis* CuZnSOD, or 86.1% of 151 aa of *X. laevis* CuZnSOD), as predicted by the Translate Tool (ExPASy, http://web.expasy.org/translate/). The 130 aa partial predicted protein sequence obtained for *R. sylvatica* CuZnSOD correspond with amino acids 3–134 of human CuZnSOD. The *R. sylvatica sod2* partial open reading frame was 393 bp, corresponding to 130 amino acids (representing 58.6% of 222 aa of human MnSOD, 58.0% of 224 aa of *X. tropicalis* MnSOD, or 58.0% of 224 aa of *X. laevis* MnSOD), as predicted by the Translate Tool (ExPASy, http://web.expasy.org/translate/). The 130 aa obtained for *R. sylvatica* MnSOD corresponds with amino acids 61–190 of human MnSOD.

A blastp search of the partial *R. sylvatica* CuZnSOD predicted protein sequence against the NCBI database showed the sequence to have 94% identity to *R. catesbeiana* CuZnSOD (GenBank accession number AC051906) and 69% identity to *X. tropicalis* CuZnSOD (GenBank accession number XP_007247311). Similarly, a blastp search of the partial *R. sylvatica* MnSOD predicted protein sequence showed the highest similarity to *X. tropicalis* MnSOD (GenBank accession number NP_001005694) with 90% identity.

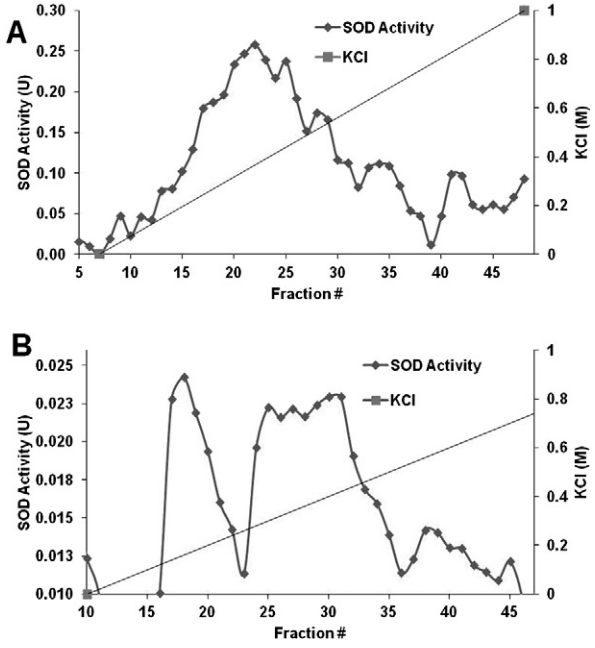


**Fig. 1.** (A) Typical elution profile for control SOD on a DEAE$^+$ column. (B) Typical elution profile for control SOD on a copper chelate column.

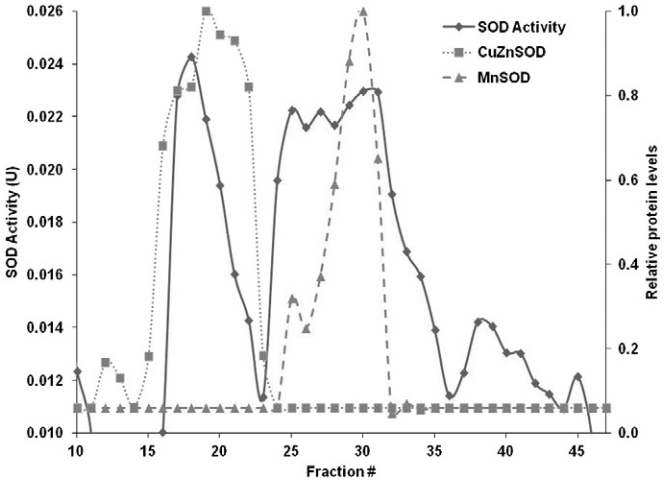


**Fig. 2.** Copper chelate column elution profile for SOD superimposed with Western blot analysis showing the presence of CuZnSOD (dotted line) or anti-MnSOD (dashed line) with enzyme activity contained within individual fractions.

Primers were designed based on the *R. sylvatica sod1* and *sod2* sequences for use in relative quantitation of mRNA levels in the muscle of control and frozen frogs. *Alpha-tubulin* was amplified from the same samples as an endogenous control. Transcript levels of *sod1* or *sod2* in the muscle of 24 h frozen frogs were not significantly different from those in the muscle of control frogs (Fig. 4A, $p > 0.05$).

### 3.4. Relative protein levels of CuZnSOD and MnSOD

Western blotting was used to evaluate the relative amount of CuZnSOD and MnSOD proteins in the muscle from control versus frozen frogs. The antibodies for CuZnSOD or MnSOD each cross-reacted with one band corresponding to the known molecular weights of ~15 kDa and ~26 kDa, for CuZnSOD and MnSOD, respectively (Fig. 3). No significant differences were detected between the protein levels in the muscle of control versus frozen frogs for either CuZnSOD or MnSOD (Fig. 4B).

### 3.5. Post-translational modification of CuZnSOD and MnSOD

To test whether or not reversible phosphorylation was the mechanism by which SOD kinetic parameters changed during anoxia,

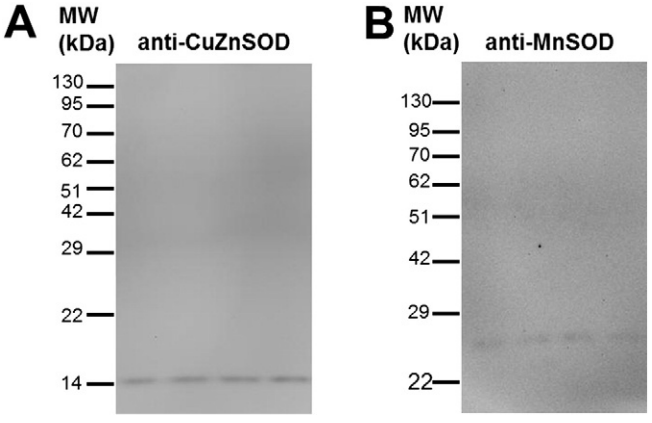


**Fig. 3.** Immunoblot analysis of (A) purified CuZnSOD and (B) purified MnSOD from the muscle of control *R. sylvatica*.

**Table 3**
CuZnSOD and MnSOD kinetic parameters from purified control and frozen *R. sylvatica* muscle.

| Enzyme parameters | Control | 24 h frozen |
|---|---|---|
| *CuZnSOD* | | |
| $K_m$ xanthine (mM) | 0.17 ± 0.02 | 0.14 ± 0.01 |
| $V_{max}$ (U/mg) | 1390 ± 10 | 2100 ± 17* |
| $C_m$ urea (M) | 0.62 ± 0.03 | 0.72 ± 0.10 |
| *MnSOD* | | |
| $K_m$ xanthine (mM) | 0.20 ± 0.01 | 0.13 ± 0.02* |
| $V_{max}$ (U/mg) | 1550 ± 85 | 1570 ± 79 |
| $C_m$ urea (M) | 2.53 ± 0.34 | 2.92 ± 0.22* |

* Indicates a significant difference from the corresponding control value, $p < 0.05$.

the fractions with the highest activity from the purification profiles for the control and frozen forms of CuZnSOD or MnSOD were combined, run on an SDS-PAGE gel, and stained with ProQ Diamond phosphoprotein stain. CuZnSOD did not react with the ProQ Diamond phosphoprotein stain, resulting in no apparent banding (data not shown). MnSOD was easily identified as a strong band found at ~23 kDa. When band densities were quantified, they showed a 2.87 fold higher band intensity ($p < 0.05$) for MnSOD from the muscle of frozen frogs when compared to the enzyme from control frogs (Fig. 5).

Immunoblotting using a dot blot apparatus was used to assess the possible differences in the amino acid-specific phosphorylation of purified muscle MnSOD between control and frozen states. Phosphorylation of serine residues of MnSOD from frozen frogs was 2.37 ± 0.37 fold higher compared to control MnSOD (1 ± 0.14, $p < 0.05$; Fig. 5). Phosphorylation via tyrosine residues of frozen MnSOD was 1.27 ± 0.05 fold higher compared to control MnSOD (1 ± 0.06, $p < 0.05$; Fig. 5). The phosphorylation levels of threonine residues between control MnSOD and frozen MnSOD did not differ ($p > 0.05$; Fig. 5).

### 3.6. Scansite prediction of phosphosites

The Scansite application from the Massachusetts Institute of Technology (http://scansite.mit.edu/) was used to analyze the obtained partial protein sequences for CuZnSOD and MnSOD for putative phosphorylation sites. Putative consensus sequences for phosphorylation sites of Erk1 kinase (threonine) and protein kinase C delta (PKC delta) (serine) were predicted for CuZnSOD (Fig. 6A, B). Putative consensus sequences for phosphorylation sites of Akt kinase (threonine), calmodulin dependent kinase 2 (threonine), casein kinase 1 (serine), Erk1 kinase (serine), PKC alpha (serine), PKC beta (serine), PKC gamma (serine), PKC delta (serine, threonine), PKC epsilon (serine, threonine), PKC zeta (serine), and PKC mu (serine, threonine) were predicted for MnSOD (Fig. 6C, D).

Human CuZnSOD was analyzed for comparison using Scansite, resulting in the following putative consensus sequences for phosphorylation sites: casein kinase 1 (threonine), PKC alpha (serine), PKC beta (serine), PKC gamma (serine), and PKC mu (serine). Human MnSOD was also analyzed using Scansite, the following putative consensus sequences for phosphorylation sites were obtained: AMP kinase (serine), calmodulin dependent kinase 2 (serine), casein kinase 1 (serine), Erk1 kinase (serine), Cdk2 kinase (serine), Cdk5 kinase (serine), PKC alpha (serine, threonine), PKC beta (serine, threonine), PKC gamma (serine, threonine), PKC delta (serine, threonine), PKC epsilon (threonine), and PKC zeta (serine). In all cases, except for casein kinase 1 for CuZnSOD, the obtained sequences for *R. sylvatica* encompassed the predicted putative phosphorylation sites for both CuZnSOD and MnSOD in humans.

### 3.7. Structural stability of CuZnSOD and MnSOD

The structural stability of CuZnSOD and MnSOD was evaluated by testing enzyme sensitivity to urea denaturation. This was evaluated by incubating muscle extracts from both control and frozen frogs for 24 h at ~4 °C in the presence of 0–7 M urea. Urea-denatured protein was then catabolized by 30 min proteolysis with thermolysin and the remaining amount of native protein was assessed by Western blotting. The calculated $C_m$ value (concentration of urea that results in a 50% loss of folded enzyme) was 0.72 M for CuZnSOD from the muscle of frozen frogs, which was not significantly different than the value of 0.62 M for CuZnSOD in control muscle extracts (Table 3; Fig. 7). The calculated $C_m$ value was 2.53 M for MnSOD from frozen frog muscle extracts, which was significantly different than the value of 2.92 M for MnSOD in control muscle extracts ($p < 0.05$) (Table 3; Fig. 8).

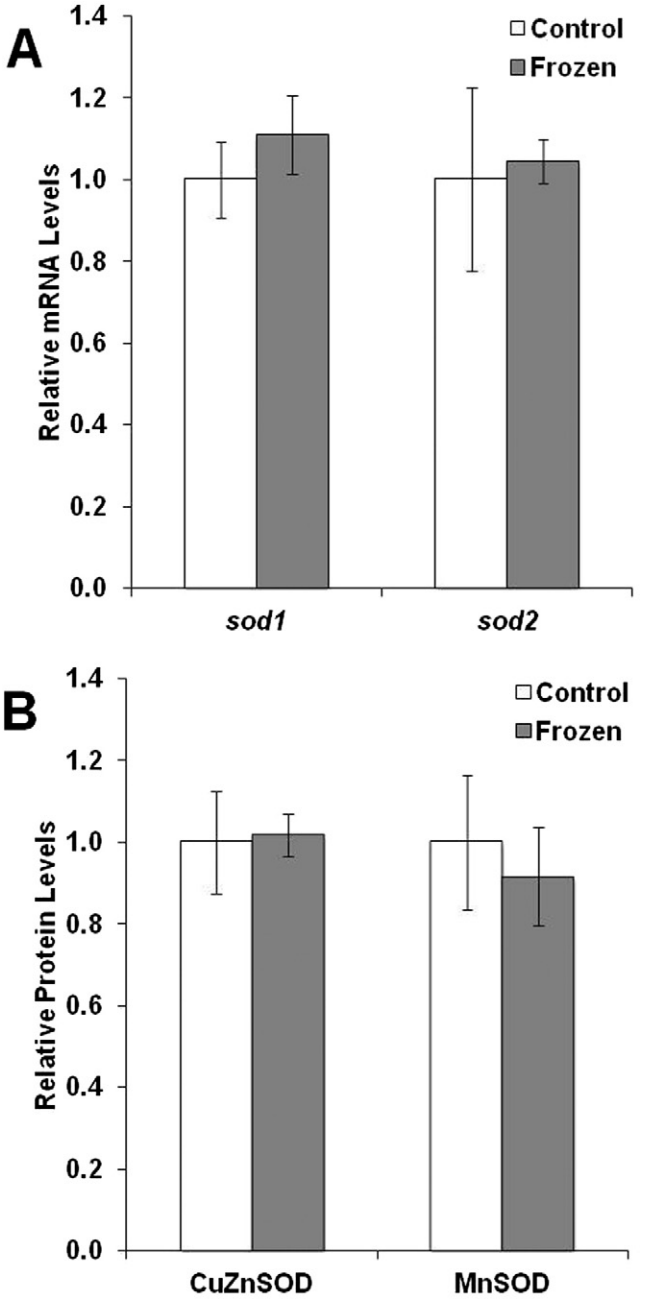


**Fig. 4.** (A) RT-PCR analysis of *sod* transcript levels in frog muscle. (B) Western blotting analysis of the relative levels of SOD proteins in frog muscle. No significant differences were observed using the Student's *t*-test ($n = 4$, $p > 0.05$).

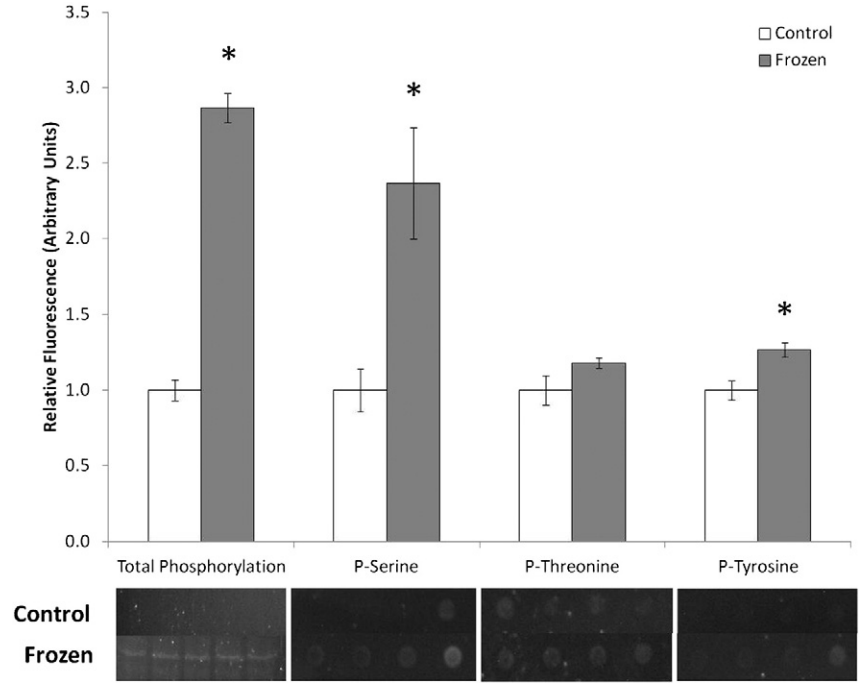


**Fig. 5.** Relative phosphorylation levels of MnSOD from the muscle of control and 24 h frozen frogs using Pro-Q Diamond phosphoprotein staining to analyze relative total phosphorylation of the enzyme, and dot-blot analysis of residue-specific phosphorylation. Data are mean ± s.e.m. and differences were analyzed by a Student's *t*-test. *Significantly different from the corresponding control value, $p < 0.05$.

## 4. Discussion

SODs are ubiquitous among living organisms and protect organisms from superoxide radicals that can oxidize and damage cellular macromolecules [34–36]. Diverse human disease states are associated with abnormalities in the structure, function or levels of SOD including: several forms of anemia, thalassemia, molecular dystrophy, cystic fibrosis, dengue fever, lateral sclerosis, rheumatoid arthritis, ischemic injury, Parkinson's disease, Alzheimer's disease and cancer [37–47]. Many of the diseases mentioned above have in common fluctuations in oxygen levels or a reduction in blood flow. To identify the importance of SOD action in both normal and disease states, various experimental approaches have been used such as knockout experiments [14,17,18]. These have had varying success; for example, *sod2* knockout experiments with animals are uniformly lethal, making it difficult to assess the role of MnSOD in the disease state [14,48]. Alternatively, the study of animals that can withstand extreme conditions can provide insight into the behavior and properties of CuZnSOD and MnSOD. In the case of freeze-

**A** **CuZnSOD**

KAGCVMKG**S**SEVTGVVRFEQEEDGPV**T**VTGQITGLTDGKHGFHIHTYGDN
TNGCVSAGPHFNPQGKTHGGPDDEVRHVGDLGNITSAAGVADINIKDKLI
CLTGEHSIVGRTAVVHEKEDDLGKGGDNES

**B**

**S** – PKC delta
**T** – Erk1 Kinase

**C** **MnSOD**

AEEKYAEALAKGDVTAQVSLQPALKFNGGGHVNHSIFWTNL**S**PSGGGEPQ
GELLKAI**T**RDFG**S**FEKFKDKL**TT**MSVAVQG**S**GWGWLGYNKESNRLQVIAC
ANQDPLQGTTGLIPLLGIDVWEHAYYLQYK

**D**

**S(1)** – Erk1 kinase
**S(2)** – PKC alpha/beta/gamma/zeta, Calmodulin dependent kinase 2
**S(3)** – PKC epsilon/delta/mu, Casein kinase 1
**T(1)** – PKC mu
**T(2)** – PKC epsilon/delta
**T(3)** – Calmodulin dependent kinase 2, Akt kinase

**Fig. 6.** Predicted phosphorylation sites for CuZnSOD and MnSOD. (A) Partial amino sequence for CuZnSOD, highlighting predicted phosphorylation sites (bold, underlined). (B) Kinases predicted to phosphorylate CuZnSOD at the amino acid sites highlighted in panel A. (C) Partial amino sequence for MnSOD, highlighting predicted phosphorylation sites (bold, underlined). (D) Kinases predicted to phosphorylate MnSOD at the amino acid sites highlighted in panel C.

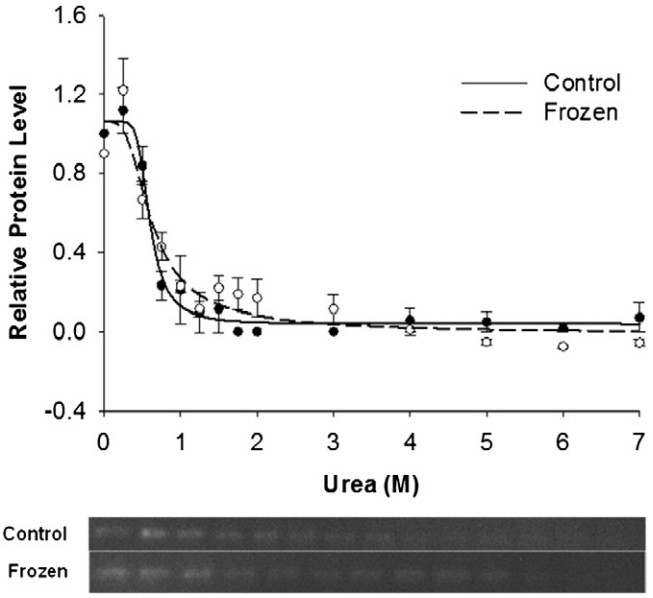


**Fig. 7.** Stability of CuZnSOD from crude extracts of frog muscle. Samples were incubated for 24 h at 4 °C with varying concentrations of urea then treated with pulse proteolysis to digest denatured CuZnSOD. Samples were then analyzed by Western blotting and band densities of urea-treated samples are plotted relative to the initial band densities of untreated enzyme samples.

tolerance, ischemic stress is imposed on the cells of *R. sylvatica* [49]. The link between free radical production in disease-induced and naturally occurring ischemic events has been widely characterized, from oxidative stress experienced during the ischemic episode, to the burst production of ROS upon re-oxygenation during reperfusion [50–52]. It is clear from these studies that SOD plays a unique role in an animal's ability to overcome stressful conditions, and the data presented in this study coincide with previous findings and further suggest another level of complexity in the mitigation of free radical damage sustained by overwintering frogs.

### *4.1. Kinetic changes of CuZnSOD and MnSOD during freezing*

The kinetic properties of wood frog skeletal muscle SODs changed significantly between control and frozen conditions, indicating possible regulation during freezing. CuZn and Mn SODs were explored independently and in a purified state; CuZnSOD exhibited a 1.52 fold higher maximal activity in the muscle of frozen frogs in comparison to control frogs, whereas MnSOD showed no change in maximal activity during freezing.

An increased CuZnSOD activity could allow for increased cytoplasmic superoxide scavenging potential during freezing, as well as during reperfusion. In the case of MnSOD, the reduction in the apparent $K_m$ of xanthine would suggest that MnSOD has a higher affinity for $O_2^{-\bullet}$, generated by the xanthine dehydrogenase reaction, during freezing. An increase in affinity for superoxide would increase the scavenging ability of MnSOD, and increase the protection against the formation of superoxide at a major site of production, the mitochondria. Mitochondrial superoxide production has been shown to trigger apoptosis, while cytosolic production of $O_2^{-\bullet}$ has been linked to many cell signaling events [53]. This would suggest that CuZnSOD is more likely to have a role in regulating cell signaling events, whereas MnSOD is more likely to have a role in keeping $O_2^{-\bullet}$ levels in the mitochondria low, staving off apoptotic cell death. This is of special interest to wood frogs since the muscle tissue thaws later than internal organs such as the heart or liver [54]. Since muscle thaws last in *R. sylvatica* during the spring thaw, rapid and successful disproportionation of $O_2^{-\bullet}$ would aid a rapid recovery of muscle functionality.

### *4.2. Regulation of CuZnSOD and MnSOD transcript and protein levels during freezing*

The stable mRNA and protein levels of CuZnSOD and MnSOD highlight the probable importance of kinetic modification of both forms of SOD during freezing as a means of adjusting SOD functionality. During periods of stress, like freezing, it is more energetically favorable to modify existing enzymes to achieve a more active state than to synthesize new enzymes de novo [55–57]. Additionally, SOD activity levels have already been shown to be more than three times greater in *R. sylvatica* muscle when compared to *Rana pipiens*, a freeze intolerant frog [4]. This may be sufficient to overcome $O_2^{-\bullet}$ production produced by freezing and subsequent thawing in conjunction with the increase in $O_2^{-\bullet}$ affinity outlined in this study.

### *4.3. Phosphorylation of CuZnSOD and MnSOD*

The lack of phosphorylation of CuZnSOD suggests that the $V_{max}$ difference observed for CuZnSOD during freezing is not controlled by reversible phosphorylation. $V_{max}$ changes can arise for many reasons, one of which may be a result of allosteric regulation. Although no mechanism for control is proposed in this manuscript, allosteric regulation of CuZnSOD has been proposed in disease states, such ALS and lateral sclerosis, to change the activity of CuZnSOD [58,59]. It is unclear at this time what caused the change in $V_{max}$ for CuZnSOD during freezing in the wood frog, although the changes remain an important point of investigation for future studies.

In contrast to CuZnMOD, MnSOD had significantly higher levels of global phosphorylation levels (2.87 fold) between control and frozen states, as well as significant increases in the relative phosphorylation of serine (2.37 fold) and tyrosine (1.27 fold) residues (Fig. 5). This suggests that the phosphorylation of MnSOD is a strong candidate for eliciting the increase in affinity for superoxide. Although it is impossible to discern the exact cause of the change in phosphorylation, it is clear that the more phosphorylated from of MnSOD is more active. Increased affinity for $O_2^{-\bullet}$ would likely enable MnSOD from the frozen frog to prevent freeze-induced free radical damage, as well as prepare for the eventual burst production of free radicals during reperfusion.

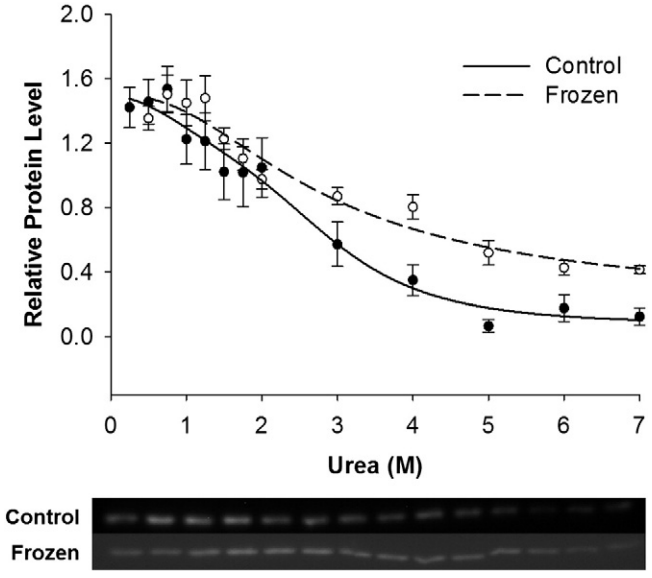


**Fig. 8.** Stability of MnSOD from crude extracts of frog muscle. Samples were incubated for 24 h at 4 °C with varying concentrations of urea then treated with pulse proteolysis to digest denatured MnSOD. Samples were then analyzed by Western blotting and band densities of urea-treated samples are plotted relative to the initial band densities of untreated enzyme samples. Frozen MnSOD showed a significant difference when compared to MnSOD from control frogs as observed using Student's *t*-test ($n = 4$, $p < 0.05$).

Previous studies have shown that levels of IP3, a second messenger of PKC, increase as freezing progresses [20], adding credence to the possibility that SOD may be controlled by phosphorylation, and that it may be phosphorylated by PKC. Investigation into the putative phosphorylation sites of MnSOD, based on the predicted protein sequence yielded several PKC phosphorylation sites, supporting PKC as a candidate to phosphorylate MnSOD during freezing. Interestingly, human MnSOD also demonstrated a larger number of potential PKC phosphorylation sites, suggesting the possibility for PKC mediated phosphorylation in humans.

### 4.4. Stability of CuZnSOD and MnSOD

When comparing CuZnSOD and MnSOD, it is clear that MnSOD is far more resistant to urea denaturation in comparison to CuZnSOD. Upon closer observation of the tertiary structure of both CuZnSOD and MnSOD from *X. laevis*, it can be seen that MnSOD has more structured regions than CuZnSOD that may lead to its apparent greater stability [13,60]. Greater stability may aid MnSOD as it is found at a major site of superoxide production, the mitochondria. Furthermore, MnSOD did show a significantly different $C_m$ between control and frozen muscle, suggesting a more stable form of MnSOD in the frozen state (Fig. 8). Covalent modifications of proteins can result in either a more rigid or a more fluid structure. There is evidence of a correlation between phosphorylation events and a subsequent stabilization of protein, as has previously been seen for the enzymes hexokinase, creatine kinase and glucose-6-phosphate dehydrogenase in *R. sylvatica* [25–27]. Covalent modification via phosphorylation may also increase accessibility of the active site, which can affect kinetic parameters. The observed phosphorylation events of MnSOD may then be affecting stability as well as increasing accessibility to the active site, thereby increasing the affinity for $O_2^{-\bullet}$ in response to freezing.

### 4.5. Conclusion

The regulation of SOD in the freeze tolerant frog, *R. sylvatica*, can provide useful insights into the effects of ischemia on free radical mediation. CuZnSOD may have increased capacity to deal with free radical production, although the exact mechanism of control is not understood. MnSOD from frozen frogs has a lower $K_m$, is more stable, and exhibits increased phosphorylation at serine and tyrosine residues as compared with MnSOD from control frogs. This study suggests a correlation between the phosphorylation of MnSOD and a decreased $K_m$ of xanthine. The evidence presented herein suggests that phosphorylation may stabilize and activate MnSOD during freezing. Augmented MnSOD activity may increase the ability of *R. sylvatica* to overcome oxidative stress associated with ischemia. This study may also provide valuable insight into disease pathology by offering a unique observation of the role of MnSOD during ischemia as *R. sylvatica* MnSOD has a high sequence identity (84%) and similar PKC phosphorylation sites as human MnSOD. This striking similarity suggests that researchers should explore possible phosphorylation events of SODs in human disease states as a method for reactivating MnSOD mutants, or in the case of ischemic tumor growth, exploring the possibility of deactivating MnSOD via de-phosphorylation as a method of triggering apoptosis.

## Acknowledgements

The authors thank Janet M. Storey for assistance in editing this manuscript. This research was supported by a discovery grant from the Natural Sciences and Engineering Research Council of Canada (NSERC) (6793 to KBS). NJD was supported by an Ontario Graduate Scholarship and BAK was supported by a NSERC post-doctoral fellowship.

## References

[1] K.B. Storey, Life in a frozen state: adaptive strategies for natural freeze tolerance in amphibians and reptiles, Am. J. Physiol. 258 (1990) R559–R568.
[2] B. Rubinsky, C.Y. Lee, J. Bastacky, J. Onik, The process of freezing and the mechanism of damage during hepatic cryosurgery, Cryobiology 27 (1987) 85–97.
[3] K.J. Cowan, K.B. Storey, Freeze–thaw effects on metabolic enzymes in wood frog organs, Cryobiology 43 (2001) 32–45.
[4] D.R. Joanisse, K.B. Storey, Oxidative damage and antioxidants in *Rana sylvatica*, the freeze-tolerant wood frog, Am. J. Physiol. 271 (3) (1996) R545–R553.
[5] B.J. Sinclair, J.R. Stinziano, C.M. Williams, H.A. MacMillan, K.E. Marshall, K.B. Storey, Real-time measurement of metabolic rate during freezing and thawing of the wood frog, *Rana sylvatica*: implications for overwinter energy use, J. Exp. Biol. 216 (2013) 292–302.
[6] K.C. Ryan, O.E. Johnson, D.E. Cabelli, T.C. Brunold, M.J. Maroney, Nickel superoxide dismutase: structural and functional roles of Cys2 and Cys6, J. Biol. Inorg. Chem. 15 (5) (2010) 795–807.
[7] J.V. Bannister, W.H. Bannister, G. Rotilio, Aspects of the structure, function, and applications of superoxide dismutase, CRC Crit. Rev. Biochem. 22 (2) (1987) 111–180.
[8] I. Fridovich, Superoxide dismutases, Annu. Rev. Biochem. 44 (1975) 147–159.
[9] S. Ahmad, C.A. Pritsos, S.M. Bowen, C.R. Heisler, G.J. Blomquist, R.S. Pardini, Subcellular distribution and activities of superoxide dismutase, catalase, glutathione peroxidase, and glutathione reductase in the southern armyworm, *Spodoptera eridania*, Arch. Insect Biochem. Physiol. 7 (1988) 173–186.
[10] M.E. Schinina, D. Barra, F. Bossa, L. Calabrese, L. Montesano, M.T. Carri, P. Mariottini, F. Amaldi, G. Rotilio, Primary structure from amino acid and cDNA sequences of two Cu, Zn superoxide dismutase variants from *Xenopus laevis*, Arch. Biochem. Biophys. 272 (1989) 507–515.
[11] S.L. Klein, R.L. Strausberg, L. Wagner, J. Pontius, S.W. Clifton, P. Richardson, Genetic and genomic tools for *Xenopus* research: the NIH *Xenopus* initiative, Dev. Dyn. 225 (4) (2002) 384–391.
[12] N.J. Hudson, S.A. Lehnert, A.B. Ingham, B. Symonds, C.E. Franklin, G.S. Harper, Lessons from an estivating frog: sparing muscle protein despite starvation and disuse, Am. J. Physiol. 290 (3) (2005) R836–R843.
[13] M. Purrello, C. Di Pietro, M. Ragusa, A. Pulvirenti, R. Giugno, V.D. Pietro, G. Emmanuele, S. Travali, M. Scalia, D. Shasha, A. Ferro, In vitro and in silico cloning of *Xenopus laevis* SOD2 cDNA and its phylogenetic analysis, DNA Cell Biol. 24 (2005) 111–116.
[14] J.E. Kokoszka, P. Coskun, L.A. Esposito, D.C. Wallace, Increased mitochondrial oxidative stress in the Sod2 (+/−) mouse results in the age-related decline of mitochondrial function culminating in increased apoptosis, Proc. Natl. Acad. Sci. U. S. A. 98 (2001) 2278–2283.
[15] B.P. Yu, Cellular defences against damage from reactive oxygen species, Physiol. Rev. 74 (1994) 139–162.
[16] R. Noor, S. Mittal, J. Iqbal, Superoxide dismutase — applications and relevance to human diseases, Med. Sci. Monit. 8 (9) (2002) RA210–RA215.
[17] C.J. Scott, E.A. Seidler, L.A. Levin, Cell-autonomous generation of mitochondrial superoxide is a signal for cell death in differentiated neuronal precursor cells, Brain Res. 1306 (2010) 142–148.
[18] Y. Li, T.T. Huang, E.J. Carlson, S. Melov, P.C. Ursell, J.L. Olson, L.J. Noble, M.P. Yoshimura, C. Berger, P.H. Chan, D.C. Wallace, C.J. Epstein, Dilated cardiomyopathy and neonatal lethality in mutant mice lacking manganese superoxide dismutase, Nat. Genet. 11 (4) (1995) 376–381.
[19] A. Duttaroy, A. Paul, M. Kundu, A. Belton, A Sod2 null mutation confers severely reduced adult life span in *Drosophila*, Genetics 165 (4) (2003) 2295–2299.
[20] C.P. Holden, K.B. Storey, Signal transduction, second messenger, and protein kinase responses during freezing exposure in wood frogs, Am. J. Physiol. 271 (1996) R1205–R1211.
[21] M.H. Rider, N. Hussain, S. Horman, S.M. Dilworth, K.B. Storey, Stress-induced activation of the AMP-activated protein kinase in the freeze-tolerant frog *Rana sylvatica*, Cryobiology 53 (2006) 297–309.
[22] S.C. Greenway, K.B. Storey, Activation of mitogen-activated protein kinases during natural freezing and thawing in the wood frog, Mol. Cell. Biochem. 209 (1999) 29–37.
[23] J.A. MacDonald, K.B. Storey, Protein phosphatase response during freezing and thawing in wood frogs: control of liver cryoprotectant metabolism, Croy-Letters 20 (1999) 297–306.
[24] J. Abboud, K.B. Storey, Novel control of lactate dehydrogenase from the freeze tolerant wood frog: role of posttranslational modifications, PeerJ 1 (2013) e12.
[25] C.A. Dieni, K.B. Storey, Regulation of hexokinase by reversible phosphorylation in skeletal muscle of a freeze tolerant frog, Comp. Biochem. Physiol. B 159 (2011) 236–243.
[26] C.A. Dieni, K.B. Storey, Regulation of glucose-6-phosphate dehydrogenase by reversible phosphorylation in liver of a freeze tolerant frog, J. Comp. Physiol. B. 180 (2010) 1133–1142.
[27] C.A. Dieni, K.B. Storey, Creatine kinase regulation by reversible phosphorylation in frog muscle, Comp. Biochem. Physiol. B 152 (2009) 405–412.
[28] C.A. Dieni, K.B. Storey, Regulation of 5′-adenosine monophosphate deaminase in the freeze tolerant wood frog, *Rana sylvatica*, BMC Biochem. 9 (2008) 12.
[29] J.N. De Croos, J.D. McNally, F. Palmieri, K.B. Storey, Upregulation of the mitochondrial phosphate carrier during freezing in the wood frog *Rana sylvatica*: potential roles of transporters in freeze tolerance, J. Bioenerg. Biomembr. 36 (2004) 229–239.
[30] B.A. Katzenback, H.A. Holden, J. Falardeau, C. Childers, H. Hadj-Moussa, T.J. Avis, K.B. Storey, Regulation of the *Rana sylvatica* brevinin-1SY antimicrobial peptide during development and in dorsal and ventral skin in response to freezing, anoxia, and dehydration, J. Exp. Biol. 217 (2014) 1392–1401.

[31] S.P. Brooks, A simple computer program with statistical tests for the analysis of enzyme kinetics, Biotechniques 13 (6) (1992) 906–911.
[32] N.J. Dawson, R.A. Bell, K.B. Storey, Purification and properties of white muscle lactate dehydrogenase from the anoxia-tolerant turtle, the red-eared slider, *Trachemys scripta elegans*, Enzyme Res. 2013 (2013) 784973.
[33] C. Park, S. Marqusee, Pulse proteolysis: a simple method for quantitative determination of protein stability and ligand binding, Nat. Methods 2 (2005) 207–212.
[34] I. Fridovich, Superoxide radical and superoxide dismutase, Ann. Rev. Biochem. 64 (1995) 97–112.
[35] J.M. McCord, Superoxide radical, controversies, contradictions and paradoxes, Proc. Soc. Exp. Biol. Med. 209 (1995) 112–117.
[36] J. Iqbal, L.B. Clerch, M.A. Hass, L. Frank, D. Massaro, Endotoxin increases lung Cu, Zn superoxide dismutase mRNA: $O_2$ raises enzyme synthesis, Am. J. Physiol. 257 (1989) L61–L64.
[37] L.F. Panchenko, T. Lamchingiin, A.M. Gerasimov, I.S. Sukhanov, L.A. Konoplin, Superoxide dismutase activity in the blood of children with iron deficiency anemia, Vopr. Med. Khim. 25 (2) (1979) 181–185.
[38] I. Mavelli, M.R. Ciriolo, L. Rossi, T. Meloni, G. Forteleoni, A. De Flora, U. Benatti, A. Morelli, G. Rotilio, Favism: a hemolytic disease associated with increased superoxide dismutase and decreased glutathione peroxidase activities in red blood cells, Eur. J. Biochem. 139 (1984) 13–18.
[39] Y. Mizuno, Superoxide dismutase activity in early stages of development in normal and dystrophic chickens, Life Sci. 34 (1984) 909–914.
[40] A. Ratoviski, P.N. Leigh, Cu/Zn superoxide dismutase gene mutations in amyotrophic lateral sclerosis: correlation between genotypes and clinical features, J. Neurol. Neurosurg. Psychiatry 61 (1996) 565–572.
[41] A. Concetti, P. Massei, G. Rotilio, M. Brunori, E.A. Rachmilewitz, Superoxide dismutase in red blood cells: method of assay and enzyme content in normal subjects and in patients with B-thalassemia, J. Lab. Clin. Med. 87 (1976) 1057–1064.
[42] G. Ray, V. Kumar, A.V. Kapoor, A.K. Dutta, S. Batra, Status of antioxidants and other biochemical abnormalities in children with dengue fever, J. Trop. Pediatr. 45 (1999) 4–7.
[43] R. Gonzales, C. Auclair, E. Voisin, H. Gautero, D. Dhermy, P. Boivin, Superoxide dismutase, catalase and glutathione peroxidase in red blood cells from patients with malignant disease, Cancer Res. 44 (1984) 4137–4139.
[44] A.A. Stieber, J.O. Gonatas, N.K. Gonatas, Aggregation of ubiquitin and a mutant ALS-linked SOD 1 protein correlate with disease progression and fragmentation of Golgi apparatus, J. Neurol. Sci. 173 (2000) 53–62.
[45] A.L. Famulari, E.R. Marschoff, S.F. Llesuy, S. Kohan, J.A. Serra, R.O. Dominquez, M. Repetto, C. Reides, E. Sacerdote de Lustig, The antioxidant enzymatic blood profile in Alzheimer's and vascular diseases. Their association and possible assay to differentiate demented subjects and controls, J. Neurol. Sci. 141 (1996) 69–78.
[46] F.P. Zemlan, O.J. Thienhaus, H.B. Bosmann, Superoxide dismutase activity in Alzheimer's disease: possible mechanism for paired helical filament formation, Brain Res. 476 (1989) 160–162.
[47] J. Rhodin, T. Thomas, M. Bryant, E.T. Sutton, Animal model of Alzheimer-like vascular pathology and inflammatory reaction, Ann. N. Y. Acad. Sci. 903 (2000) 345–352.
[48] S. Melov, P. Coskun, M. Patel, R. Tuinstra, B. Cottrell, S. Jun, T.H. Zastawny, M. Dizdaroglu, S.I. Goodman, T.T. Huang, H. Miziorko, C.J. Epstein, C. Wallace, Mitochondrial disease in superoxide dismutase 2 mutant mice, Proc. Natl. Acad. Sci. U. S. A. 96 (1999) 846–851.
[49] K.B. Storey, J.M. Storey, Freeze tolerant frogs: cryoprotectants and tissue metabolism during freeze–thaw cycles, Can. J. Zool. 64 (1984) 49–56.
[50] R. Ferrari, C. Ceconi, S. Curello, A. Cargnoni, E. Pasini, O. Sioli, The occurrence of oxidative stress during reperfusion in experimental animals and men, Cardiovasc. Drugs Ther. 5 (1991) 277–287.
[51] P.J. Simpson, B.R. Lucchesi, Free radicals and myocardial ischemia and reperfusion injury, J. Lab. Clin. Med. 110 (1) (1987) 13–30.
[52] J.L. Zweier, M.A. Talukder, The role of oxidants and free radicals in reperfusion injury, Cardiovasc. Res. 70 (2) (2006) 181–190.
[53] V. Thannickal, B. Fanburg, Reactive oxygen species in cell signalling, Am. J. Physiol. 279 (2000) L1005–L1028.
[54] B. Rubinsky, S.T.S. Wong, J.-S. Hong, J. Gilbert, M. Roos, K.B. Storey, $^1$H magnetic resonance imaging of freezing and thawing in freeze-tolerant frogs, Am. J. Physiol. 266 (1994) R1771–R1777.
[55] K.B. Storey, Freeze tolerance in the frog, *Rana sylvatica*, Experientia 40 (1984) 1261–1262.
[56] J.M. Storey, K.B. Storey, Cold hardiness and freeze tolerance, in: K.B. Storey (Ed.), Functional Metabolism: Regulation and Adaptation, Wiley-Liss, Hoboken, 2004, pp. 473–503.
[57] K.B. Storey, Strategies for exploration of freeze responsive gene expression: advances in vertebrate freeze tolerance, Cryobiology 48 (2004) 134–145.
[58] A.D. Schuyler, H.A. Carlson, E.L. Feldman, Computational methods for identifying a layered allosteric regulatory mechanism for ALS-causing mutations of Cu–Zn superoxide dismutase 1, Proteins 79 (2) (2011) 417–427.
[59] A. Das, S.S. Plotkin, SOD1 exhibits allosteric frustration to facilitate metal binding affinity, Proc. Natl. Acad. Sci. U. S. A. 110 (10) (2013) 3871–3876.
[60] K.D. Carugo, A. Battistoni, M.T. Carri, F. Polticelli, A. Desideri, G. Rotilio, A. Coda, K.S. Wilson, M. Bolognesi, Three-dimensional structure of *Xenopus laevis* Cu, Zn superoxide dismutase b determined by X-ray crystallography at 1.5 Å resolution, Acta Crystallogr. D52 (1996) 176–188.